Appl. Math. Mech. -Engl. Ed., **44**(6), 1023–1034 (2023)

APPLIED MATHEMATICS AND MECHANICS (ENGLISH EDITION)

https://doi.org/10.1007/s10483-023-3006-9

Linear analysis of the dynamic response of a riser subject to internal solitary waves*

Dalin TAN[1,2], Xu WANG[1,†], Jinlong DUAN[1], Jifu ZHOU[1,3]

1. Key laboratory for Mechanics in Fluid Solid Coupling Systems, Institute of Mechanics, Chinese Academy of Sciences, Beijing 100190, China;
2. Beijing Electro-Mechanical Engineering Institute, Beijing 100074, China;
3. School of Engineering Sciences, University of Chinese Academy of Sciences, Beijing 100049, China

(Received Nov. 1, 2022 / Revised Apr. 21, 2023)

Abstract The flow field induced by internal solitary waves (ISWs) is peculiar wherein water motion occurs in the whole water depth, and the strong shear near the pycnocline can be generated due to the opposite flow direction between the upper and lower layers, which is a potential threat to marine risers. In this paper, the flow field of ISWs is obtained with the Korteweg-de Vries (KdV) equation for a two-layer fluid system. Then, a linear analysis is performed for the dynamic response of a riser with its two ends simply supported under the action of ISWs. The explicit expressions of the deflection and the moment of the riser are deduced based on the modal superposition method. The applicable conditions of the theoretical expressions are discussed. Through comparisons with the finite element simulations for nonlinear dynamic responses, it is proved that the theoretical expressions can roughly reveal the nonlinear dynamic response of risers under ISWs when the approximation for the linear analysis is relaxed to some extent.

Key words internal solitary wave (ISW), riser, dynamic response, linear analysis

Chinese Library Classification O352
2010 Mathematics Subject Classification 74F10

1 Introduction

Risers are widely used in connecting floating platforms on the surface and wellheads in the seabed. As the key component in the marine resource exploitation system, the stability of these risers directly determines the economic efficiency and safety of the system. Thus, the dynamic response of risers under ocean environment loads is always a forefront issue in ocean engineering.

∗ Citation: TAN, D. L., WANG, X., DUAN, J. L., and ZHOU, J. F. Linear analysis of the dynamic response of a riser subject to internal solitary waves. *Applied Mathematics and Mechanics* (*English Edition*), **44**(6), 1023–1034 (2023) https://doi.org/10.1007/s10483-023-3006-9

† Corresponding author, E-mail: wangxu@imech.ac.cn

Project supported by the National Natural Science Foundation of China (Nos. 12132018, 11972352, and 12202455) and the Strategic Priority Research Program of the Chinese Academy of Sciences of China (No. XDA22000000)

A large number of observations showed that internal solitary waves (ISWs) occur frequently and exist widely in the ocean due to the density stratification arising from salinity and temperature variations[1]. ISWs can cause severe impacts on the operation of ocean engineering structures[2], and even lead to cable breakage as occurred in the extended test period of the Liuhua Oilfield in the South China Sea[3]. There is no doubt that the strong currents induced by ISWs are a potential threat to submerged structures.

Therefore, many studies have been carried out to investigate the hydrodynamic forces exerted by ISWs on cylindrical piles. For example, Cai et al.[4–5] introduced the Morison empirical method, modal separation, and regression analyses to estimate the forces and torques exerted on the cylindrical piles by the ISWs. It was found that the forces exerted by the ISWs were much larger than those caused due to the surface wave. Xie et al.[6] used a numerical model to study the time-dependent load on cylindrical piles by an ISW packet in a continuously stratified ocean. Lü et al.[7] conducted several numerical experiments to study the impacts of background current on the force and torque exerted by the ISWs on a small-diameter cylindrical tension leg of the oil platform. With respect to dynamic response issues, Song et al.[8] developed a time-domain numerical model to compute the action of the ISWs on marine structures and structure motion responses. Guo et al.[9] investigated the dynamic response of a top tensioned riser under the combined excitation of the ISW, the surface wave, and the vessel motion by numerical simulation. Fan et al.[10] found that the envelopes of riser properties in the upper layer and the horizontal deviation of a hang-off riser bottom dramatically increased under the effect of ISWs. Lou et al.[11] proposed a dynamic model for steel catenary risers (SCRs) based on the principle of virtual work, where the equations of motion were obtained by combining Euler's equation and the initial conditions. Overall, most of the previous works on the interaction between the risers and ISWs are carried out by means of numerical simulation or laboratory experiments. Analytical research has been rare on this issue.

In this paper, linear analysis is implemented to examine the dynamic response of risers under ISWs via the modal superposition method. Section 2 introduces the general expression of dynamic responses on a riser. Then, the dynamic response of a riser under ISWs is analyzed by a linear approach with a series of reasonable approximations in Section 3. Some discussion is given in Section 4. Finally, conclusions are drawn.

2 Theoretical derivation

2.1 General expression of dynamic responses of a riser

Undergoing horizontal bending loads, such as winds, currents, and waves, risers with the characteristic of a high length-to-diameter ratio are generally treated as beam structures. Figure 1 shows the sketch of a beam structure under a dynamic load, where $p(z,t)$ indicates the dynamic distributed load, and H indicates the length of the beam structure. The deflection of the beam can be expressed as

$$v(z,t)=\sum_{s=1}^{\infty}V_s(z)q_s(t),$$

where $V_s(z)$ is the vibration mode function of the sth-order mode, and $q_s(t)$ is the generalized deflection of the sth-order mode. Then, the kinetic energy of this beam can be written as

$$T=\frac{1}{2}\int_0^H\rho A(z)\Big(\frac{\partial v}{\partial t}\Big)^2\mathrm{d}z=\frac{1}{2}\sum_i\sum_j\int_0^H\rho A(z)V_i(z)V_j(z)\mathrm{d}z\cdot\dot{q}_i(t)\dot{q}_j(t)=\frac{1}{2}\sum_{s=1}^{\infty}m_s\dot{q}_s^2, \quad (1)$$

where $A(z)$ is the transversal area of the beam structure, m_s is the generalized mass of the sth-order mode, and i and j denote the generalized coordinates. The elastic potential energy

can be written as

$$P = \frac{1}{2}\int_0^H EI(z)\Big(\frac{\partial^2 v}{\partial z^2}\Big)^2 \mathrm{d}z$$
$$= \frac{1}{2}\sum_i \sum_j \int_0^H EI(z)V_i''(z)V_j''(z)\mathrm{d}z \cdot q_i(t)q_j(t) = \frac{1}{2}\sum_{s=1}^{\infty} m_s\omega_s^2 q_s^2, \tag{2}$$

where E is the elastic modulus, $I(z)$ is the cross-sectional moment of inertia, and ω_s is the vibration frequency of the sth-order mode. The virtual work of $p(z,t)$ is

$$\delta W = \int_0^H (p(z,t)\mathrm{d}z \cdot \delta v) = \int_0^H p(z,t)\sum_s V_s(z)\delta q_s \mathrm{d}z$$
$$= \sum_s (p(z,t)V_s(z)\mathrm{d}z)\delta q_s = \sum_{s=1}^{\infty} Q_s(t)\delta q_s, \tag{3}$$

where $Q_s(t)$ is the generalized force, representing the work of the dynamic force in the vibration mode function of the sth-order mode.

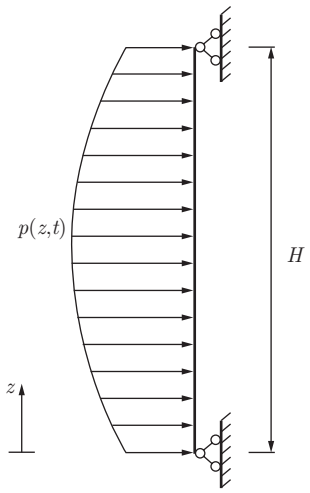

Fig. 1 Schematic of the beam structure under a distributed load

Substituting Eqs. (1)–(3) into the Lagrange equation yields

$$\frac{\mathrm{d}}{\mathrm{d}t}\Big(\frac{\partial T}{\partial q_s}\Big) - \frac{\partial (T-P)}{\partial q_s} = Q_s, \quad s = 1, 2, 3, \cdots. \tag{4}$$

Thus, the dynamic response equation of the beam structures is

$$m_s\ddot{q}_s(t) + m_s\omega_s^2 q_s(t) = Q_s(t), \quad s = 1, 2, 3, \cdots \tag{5}$$

with the initial deflection q_{s0} and the velocity $\dot{q}_{s0}$. The time-dependent deflection can be expressed as

$$q_s(t) = q_{s0}\cos(\omega_s t) + \frac{\dot{q}_{s0}}{\omega_s}\sin(\omega_s t) + \frac{e_s(t)}{m_s\omega_s}, \quad s = 1, 2, 3, \cdots, \tag{6}$$

where $e_s(t)$ is the generalized impulse defined as

$$e_s(t) = \int_0^t Q_s(\tau)\sin(\omega_s(t-\tau))\mathrm{d}\tau. \tag{7}$$

The deflection and the moment of the beam can be written as

$$v(z,t) = \sum_{s=1}^{\infty}\Big(q_{s0}\cos(\omega_s t) + \frac{\dot{q}_{s0}}{\omega_s}\sin(\omega_s t) + \frac{e_s(t)}{m_s\omega_s}\Big)\cdot V_s(z), \tag{8}$$

$$M(z,t) = EI(z)\cdot\sum_{s=1}^{\infty}\Big(q_{s0}\cos(\omega_s t) + \frac{\dot{q}_{s0}}{\omega_s}\sin(\omega_s t) + \frac{e_s(t)}{m_s\omega_s}\Big)\cdot\frac{\partial^2 V_s(z)}{\partial z^2}. \tag{9}$$

For a simply supported beam structure, the vibration frequency, the vibration mode function, and the generalized mass are, respectively,

$$\omega_s = \frac{s^2\pi^2}{H^2}\sqrt{\frac{EI}{\rho A_{\mathrm{r}}}}, \quad s = 1,2,3,\cdots, \tag{10}$$

$$V_s = \sin\Big(\frac{s\pi}{H}z\Big), \quad s = 1,2,3,\cdots, \tag{11}$$

$$m_s = \int_0^H \rho A_{\mathrm{r}}\sin^2\Big(\frac{s\pi z}{H}\Big)\mathrm{d}z = \frac{\rho A_{\mathrm{r}}H}{2}, \quad s = 1,2,3,\cdots, \tag{12}$$

where ρ and A_{r} denote the density and the cross-sectional area of the beam, respectively.

Equation (10) shows that the vibration frequencies increase by the square of the order of modes. Combined with Eqs. (8) and (9), it can be seen that the contribution of high-order modes to the global deflection and the moment is quite limited.

3 Linear analysis for the dynamic response of a riser under ISWs

By conducting a linear analysis for the dynamic response of a riser under a sinusoidally varying distributed load, the stress and the dynamic response of a simply supported riser can be revealed accurately and directly. In this section, the dynamic response of a riser under ISWs is investigated based on the above method.

3.1 Expression of ISW forces

A riser under an ISW in a two-layer fluid is considered. The coordinate system is shown in Fig. 2. The origin is placed at the bottom of the riser, and the z-axis is the central axis of the riser. The densities of the two layers are ρ_1 and ρ_2, respectively, and the thicknesses are h_1 and h_2, respectively.

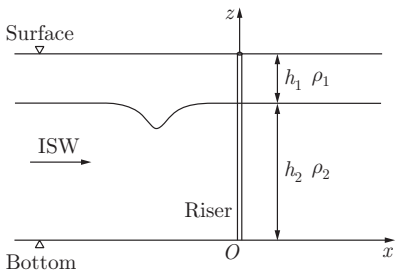

Fig. 2 Schematic of a riser under an ISW

The ISW propagating in the x-direction can be described by the following Korteweg-de Vries (KdV) equation[12]:

$$\frac{\partial \eta}{\partial t} + c_0 \frac{\partial \eta}{\partial x} + \alpha \eta \frac{\partial \eta}{\partial x} + \beta \frac{\partial^3 \eta}{\partial x^3} = 0, \tag{13}$$

where η is the vertical displacement of pycnocline from their equilibrium levels, and c_0, α, and β are the linear phase speed, the coefficient of the nonlinear term, and the dispersive term, respectively, which are expressed as follows:

$$c_0 = \sqrt{\frac{g\sigma h_1 h_2}{h_1 + h_2}}, \tag{14}$$

$$\alpha = \frac{3}{2} c_0 \frac{h_1 - h_2}{h_1 h_2}, \tag{15}$$

$$\beta = \frac{c_0}{6} h_1 h_2, \tag{16}$$

in which g is the gravitational acceleration, and $\sigma = 2(\rho_2 - \rho_1)/(\rho_1 + \rho_2)$ is the relative layer density difference.

The solitary wave solutions to the KdV equation (Eq. (13)) can be written in a number of forms[13], one of which is

$$\eta(x,t) = a\mathrm{sech}^2\left(\frac{x - c(t - \Delta t)}{\sqrt{\frac{12\beta}{\alpha A}}}\right), \tag{17}$$

where A is the wave amplitude, Δt is the initial time adjustment to ensure the vertical displacement $\eta = 0$ when $t = 0$ (Δt is a constant for a specific KdV situation, which will be ignored in the following derivations), and $c = c_0 + a\alpha/3$ denotes the wave speed. For $x = 0$ and $k = c\sqrt{\frac{\alpha A}{12\beta}}$, Eq. (17) can be written as

$$\eta(t) = A\mathrm{sech}^2(-kt), \tag{18}$$

where k is the generalized frequency of the ISW.

From the assumption that at least one of the thicknesses of the fluid layers is much smaller than the characteristic wavelength, the averaged velocity and layer thickness are related by the expression[14]

$$\overline{u}(t) = \begin{cases} \dfrac{c\eta(t)}{h_1 + \eta(t)}, & h_2 < z < h_1 + h_2, \\ -\dfrac{c\eta(t)}{h_2 - \eta(t)}, & 0 < z < h_2. \end{cases} \tag{19}$$

In typical circumstances, if the wave amplitude is a relatively small parameter compared with the thicknesses of the two layers, i.e.,

$$\eta(t)/h_1 \ll 1, \quad \eta(t)/h_2 \ll 1, \tag{20}$$

the ISW only changes the velocity of the flow fields, while the position of the pycnocline remains unchanged. Figure 3 shows that the effect of the ISW can be regarded as a time-dependent shear flow,

$$\overline{u}(t) = \begin{cases} \dfrac{c\eta(t)}{h_1}, & h_2 < z < h_1 + h_2, \\ -\dfrac{c\eta(t)}{h_2}, & 0 < z < h_2. \end{cases} \tag{21}$$

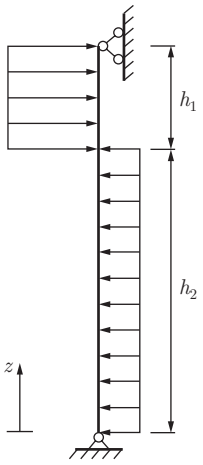

Fig. 3 Configuration of the mechanical model of a riser under the ISW

The hydrodynamic force per length on a pile exerted by the ISW can be calculated with the Morison equation[15],

$$F = C_{\mathrm{M}}\frac{\pi D^2}{4}\rho_{\mathrm{w}}\frac{\partial \overline{u}}{\partial t} + \frac{1}{2}C_{\mathrm{D}}\rho_{\mathrm{w}}D\overline{u}\,|\overline{u}|\,, \tag{22}$$

where D is the diameter of the pile, and C_{M} and C_{D} are the coefficients of the inertia force and the drag force, respectively.

For actual ISWs, the time duration of the ISW is commonly about 10–20 min, while the horizontal velocity of the flow field is about 2 m/s[16]. This means that the inertia term is much smaller than the drag term during this time frame, and Eq. (22) can be simplified as

$$F = \frac{1}{2}C_{\mathrm{D}}\rho_{\mathrm{w}}D\overline{u}\,|\overline{u}|\,. \tag{23}$$

From Eqs. (21) and (23), the acting force of the ISW on a riser can be given as

$$F = \begin{cases} \dfrac{1}{2}C_{\mathrm{D}}\rho_1 D\dfrac{c^2A^2}{h_1^2}\mathrm{sech}^4(-kt), & h_2 < z < h_1 + h_2, \\ -\dfrac{1}{2}C_{\mathrm{D}}\rho_2 D\dfrac{c^2A^2}{h_2^2}\mathrm{sech}^4(-kt), & 0 < z < h_2. \end{cases} \tag{24}$$

3.2 Linear analysis of dynamic responses

Since the density difference of the two layers is small (usually less than 1%), the average density $\rho_{\mathrm{m}} = (\rho_1 + \rho_2)/2$ is introduced to replace ρ_1 and ρ_2 in Eq. (24). Then, the generalized force of the ith-order mode can be presented as

$$Q_i(t) = \int_0^H FV_i(z)\mathrm{d}z = \int_0^H F\sin\Big(\frac{i\pi}{H}z\Big)\mathrm{d}z = f_i\cdot\mathrm{sech}^4(-kt), \quad i = 1, 2, 3, \cdots, \tag{25}$$

where f_i is a time independent parameter, which is given as

$$f_i = \frac{1}{2}C_{\mathrm{D}}\rho_{\mathrm{m}}Dc^2A^2\frac{H}{i\pi}\Big(\Big(\frac{1}{h_1^2} + \frac{1}{h_2^2}\Big)\cos\Big(\frac{i\pi h_2}{H}\Big) - \Big(\frac{(-1)^i}{h_1^2} + \frac{1}{h_2^2}\Big)\Big). \tag{26}$$

From Eq. (7), the generalized impulse can be written as

$$e_i(t) = f_i \cdot \int_0^t \operatorname{sech}^4(-kt)\sin(\omega_i(t-\tau))\mathrm{d}\tau. \tag{27}$$

It can be seen from Eq. (27) that the generalized impulse cannot be obtained by direct integration.

Here, several approximations are made in the derivation process. The second-order Taylor expansion of the natural logarithm function is introduced as follows:

$$\operatorname{sech}^4(-k\tau) = 16\mathrm{e}^{-4k\tau}\Big(\frac{1}{\mathrm{e}^{-2k\tau}+1}\Big)^4 = \mathrm{e}^{-4k\tau}(1+4k\tau+6k^2\tau^2). \tag{28}$$

Then, the generalized impulse is

$$\begin{aligned} e_i(t) = \frac{f_i}{(16k^2+\omega_i^2)^3}(&\mathrm{e}^{-4kt}(1\,536k^6\omega_i t^2 + 2\,560k^5\omega_i t + 1\,344k^4\omega_i \\ &+ 192k^4\omega_i^3 t^2 + 224k^3\omega_i^3 t + 52k^2\omega_i^3 + 6k^2\omega_i^5 t^2 + 4k\omega_i^5 t + \omega_i^5) \\ &+ \sin(\omega_i t)(2\,816k^5 - 16k^3\omega_i^2) + \cos(\omega_i t)(-1\,344k^4\omega_i - 52k^2\omega_i^3 - \omega_i^5)). \end{aligned} \tag{29}$$

After substituting Eq. (29) into Eq. (6), the expression of Eq. (6) still includes two unknown variables (the initial deflection q_{i0} and the initial velocity $\dot{q}_{i0}$). It is necessary to combine the initial condition to solve for them.

The ISW reaches its maximum amplitude at $t = 0$ (see Eq. (18)). When the time approaches infinity ($t \to \infty$), the ISW returns to its equilibrium. As a result, the induced flow fields and the time-dependent deflection $q_i(t)$ of the riser tend to be zero.

$$\begin{aligned} q_i|_{t\to\infty} = q_{i0}\cos(\omega_i t)|_{t\to\infty} + \frac{\dot{q}_{i0}}{\omega_i}\sin(\omega_i t)\Big|_{t\to\infty} + \frac{1}{m_i\omega_i}\frac{f_i}{(16k^2+\omega_i^2)^3}(&\mathrm{e}^{-4kt}(1\,536k^6\omega_i t^2 \\ + 2\,560k^5\omega_i t + 1\,344k^4\omega_i + 192k^4\omega_i^3 t^2 + 224k^3\omega_i^3 t + 52k^2\omega_i^3 + 6k^2\omega_i^5 t^2 + 4k\omega_i^5 t + \omega_i^5) \\ + \sin(\omega_i t)(2\,816k^5 - 16k^3\omega_i^2) + \cos(\omega_i t)(-1\,344k^4\omega_i - 52k^2\omega_i^3 - \omega_i^5))_{t\to\infty} = 0. \end{aligned} \tag{30}$$

When $t \to \infty$, the term e^{-4kt} in Eq. (30) approaches zero rapidly. Therefore, the variables q_{i0} and $\dot{q}_{i0}$ can be written as

$$q_{i0} = \frac{f_i}{m_i\omega_i}\frac{(1\,344k^4\omega_i + 52k^2\omega_i^3 + \omega_i^5)}{(16k^2+\omega_i^2)^3}, \tag{31}$$

$$\dot{q}_{i0} = \frac{f_i}{m_i}\frac{(-2\,816k^5 + 16k^3\omega_i^2)}{(16k^2+\omega_i^2)^3}. \tag{32}$$

Substituting Eqs. (29), (31), and (32) into Eq. (6), we can obtain the expression of time-dependent deflection $q_i(t)$ as follows:

$$\begin{aligned} q_i(t) = \frac{f_i}{m_i\omega_i}\frac{\mathrm{e}^{-4kt}}{(16k^2+\omega_i^2)^3}(&1\,536k^6\omega_i t^2 + 2\,560k^5\omega_i t + 1\,344k^4\omega_i + 192k^4\omega_i^3 t^2 \\ &+ 224k^3\omega_i^3 t + 52k^2\omega_i^3 + 6k^2\omega_i^5 t^2 + 4k\omega_i^5 t + \omega_i^5). \end{aligned} \tag{33}$$

Based on the modal superposition method, the deflection and the moment of the riser with

two simply support edges can be written as

$$\begin{aligned} v(z,t) &= \sum_{i=1}^{\infty} q_i(t)\cdot\sin\Big(\frac{i\pi z}{H}\Big) \\ &= \sum_{i=1}^{\infty}\frac{f_i}{m_i\omega_i}\frac{\mathrm{e}^{-4kt}}{(16k^2+\omega_i^2)^3}(1\,536k^6\omega_i t^2+2\,560k^5\omega_i t+1\,344k^4\omega_i+192k^4\omega_i^3t^2 \\ &\quad +224k^3\omega_i^3t+52k^2\omega_i^3+6k^2\omega_i^5t^2+4k\omega_i^5t+\omega_i^5)\sin\Big(\frac{i\pi z}{H}\Big), \end{aligned} \tag{34}$$

$$\begin{aligned} M(z,t) &= EI\sum_{i=1}^{\infty} q_i(t)\cdot\frac{\partial^2 V_i(z)}{\partial z^2} = -\frac{EI\pi^2}{H^2}\sum_{i=1}^{\infty} i^2 q_i(t)\cdot\sin\Big(\frac{i\pi z}{H}\Big) \\ &= -\frac{EI\pi^2}{H^2}\sum_{i=1}^{\infty}\frac{i^2 f_i}{m_i\omega_i}\frac{\mathrm{e}^{-4kt}}{(16k^2+\omega_i^2)^3}(1\,536k^6\omega_i t^2+2\,560k^5\omega_i t+1\,344k^4\omega_i \\ &\quad +192k^4\omega_i^3t^2+224k^3\omega_i^3t+52k^2\omega_i^3+6k^2\omega_i^5t^2+4k\omega_i^5t+\omega_i^5)\sin\Big(\frac{i\pi z}{H}\Big). \end{aligned} \tag{35}$$

For the KdV solitary waves, their wavelength $L_{\mathrm{w}}=2/k$[16]. In the actual sea, the wavelength of the ISW is always kilometer-scale. Hence, the magnitude of k can be regarded as $k\leqslant 10^{-3}$. If the vibration frequency of the riser $\omega_i>10^{-1}$, which means that the absolute value is much larger than k, the deflection (Eq. (34)) and the moment (Eq. (35)) of the riser with two simply supported edges can be further simplified as

$$v(z,t)=\sum_{i=1}^{\infty} q_i(t)\cdot\sin\Big(\frac{i\pi z}{H}\Big)=\sum_{i=1}^{\infty}\frac{f_i}{m_i}\frac{\mathrm{e}^{-4kt}}{\omega_i^2}\sin\Big(\frac{i\pi z}{H}\Big), \tag{36}$$

$$M(z,t)=EI\sum_{i=1}^{\infty} q_i(t)\cdot\frac{\partial^2 V_i(z)}{\partial z^2}=-\frac{EI\pi^2}{H^2}\sum_{i=1}^{\infty} i^2\frac{f_i}{m_i}\frac{\mathrm{e}^{-4kt}}{\omega_i^2}\cdot\sin\Big(\frac{i\pi z}{H}\Big). \tag{37}$$

The applicable condition of Eqs. (36) and (37) is $\omega_i>10^{-1}$. According to Eq. (10), the length of the riser should be satisfied by

$$H<\pi\Big(\frac{100EI}{\rho A_{\mathrm{r}}}\Big)^{\frac{1}{4}}. \tag{38}$$

From Eq. (36), the deflection $v(z,t)$ reaches a maximum when $t=0$, which implies that the maximum values of the deflection and the moment appear concurrent with the wave peak/trough of ISWs (see Eq. (18)),

$$v(z)|_{\max}=\sum_{i=1}^{\infty} q_i(t)\cdot\sin\Big(\frac{i\pi z}{H}\Big)=\sum_{i=1}^{\infty}\frac{f_i}{m_i\omega_i^2}\sin\Big(\frac{i\pi z}{H}\Big), \tag{39}$$

$$M(z,t)|_{\max}=EI\sum_{i=1}^{\infty} q_i(t)\cdot\frac{\partial^2 V_i(z)}{\partial z^2}=-\frac{EI\pi^2}{H^2}\sum_{i=1}^{\infty} i^2\frac{f_i}{m_i\omega_i^2}\sin\Big(\frac{i\pi z}{H}\Big). \tag{40}$$

For a specific circumstance, the terms f_i, m_i, and $\sin\big(\frac{i\pi z}{H}\big)$ in Eq. (36) are known. e^{-4kt} and ω_i^2 are the main influencing factors. Specifically, the variable k determines the duration of the dynamic responses, and ω_i significantly impacts the amplitude of the deflection.

4 Discussion

The foregoing theory describes the linear dynamic response of a riser under the ISWs. In this section, the effects of the wave amplitude on the dynamic response are investigated based

on a comparison between the numerical results by the ABAQUS platform and the theoretical results of the present linear analysis. The implicit dynamics method is adopted during the ABAQUS simulation. The pile is discretized into 1 400 beam elements, and the fixed time step is set to be 10 s (the total time of simulation is 4 000 s).

Table 1 shows the parameters of the riser and hydrodynamics used in the subsequent sections.

Table 1 Parameters of the riser and hydrodynamics

Riser parameter	Value	Hydrodynamic parameter	Value
Elasticity modulus E/GPa	210	Thickness of upper layer h_1/m	150/200/250
Shear modulus G/GPa	81	Thickness of lower layer h_2/m	550/500/450
Diameter D/m	0.3	Density of upper layer $\rho_1/(\mathrm{kg}\cdot\mathrm{m}^{-3})$	1 020
Thickness of riser t/m	0.02	Density of lower layer $\rho_2/(\mathrm{kg}\cdot\mathrm{m}^{-3})$	1 030
Density of riser $\rho/(\mathrm{kg}\cdot\mathrm{m}^{-3})$	7 850	Drag coefficient C_D	1.0
Length of riser H/m	700		
Unit weight $w/(\mathrm{N}\cdot\mathrm{m}^{-1})$	643		

Figure 4 shows the deflection (here, we define ν/D as the dimensionless deflection of a riser) of the linear analysis and the numerical simulation (ABAQUS) when the maximum deflection occurs ($t = 0$) for $h_1 = 250\,\mathrm{m}$, $H = 700\,\mathrm{m}$, and $A = -15\,\mathrm{m}$. Here, the length of the riser H satisfies the condition of Eq. (37), and thus the simplified formulae, i.e., Eqs. (35) and (36) can be used to calculate the deflection. The result shows that the deflection using the linear analysis method is in good agreement with the numerical simulation by ABAQUS. It can be seen from Fig. 4 that the maximum deflection obtained based on the linear analysis method is equal to 228.83, while the one calculated by ABAQUS is 223.93. The relative error of the results between these two methods is 1.80%. Therefore, it can be concluded that the linear analysis presented can predict the deflection of a riser under ISWs accurately with much lower computational resource consumption.

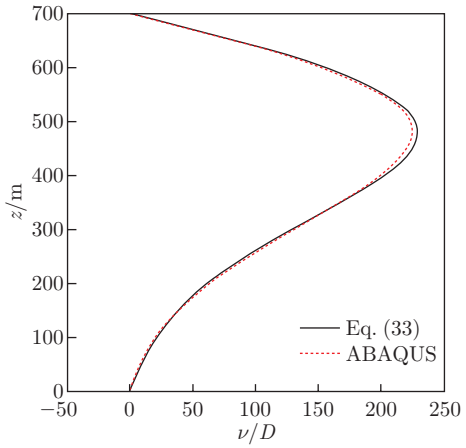

Fig. 4 Deflection of the riser using the linear analysis and numerical simulation (ABAQUS) when the maximum deflection appears for $h_1 = 250\,\mathrm{m}$, $H = 700\,\mathrm{m}$, and $A = -15\,\mathrm{m}$ (color online)

It is necessary to determine the restricted conditions for the proposed method. Here, the relationships between the amplitudes of the ISWs and the maximum deflection of a riser in different density stratifications are shown in Figs. 5–7. It is indicated that with the increase in the wave amplitude A, the deflection of the riser varies in a similar trend for the linear analysis and numerical results.

Specifically, for low wave amplitudes (about $A/h_1 \leqslant 0.1$, which meets the requirements of Eq. (20) in the process of derivation), the results agree well with each other (the relative errors are within 5%). For instance, under $A/h_1 \leqslant 0.1$, the relative errors of the maximum values of the riser deflection with $h_1/H = 150/700$, $200/700$, and $250/700$ are found equal to 5.06%, 3.81%, and 2.21%, respectively. The relative errors increase gradually when the wave amplitude increases. As shown in Figs. 5–7, the relative errors between the riser deflection by the linear analysis method and ABAQUS are increased up to 14.56%, 7.34%, and 2.88% with $h_1/H = 150/700$, $200/700$, and $250/700$ while $A/h_1 = 0.2$, 0.15, and 0.12, respectively. Although the relative errors of the riser deflection obtained based on the linear analysis method and ABAQUS show an increasing trend with the increase in the ISW amplitude, the results calculated by these two approaches show good agreement, indicating the accuracy of the linear analysis method here.

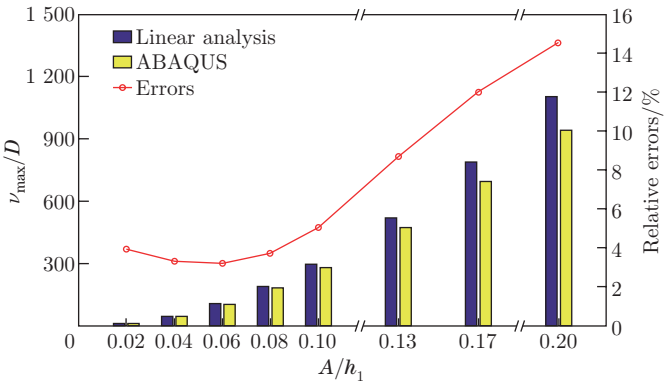

Fig. 5 Relationship between the wave amplitudes and the maximum deflection when $h_1/H = 150/700$ (color online)

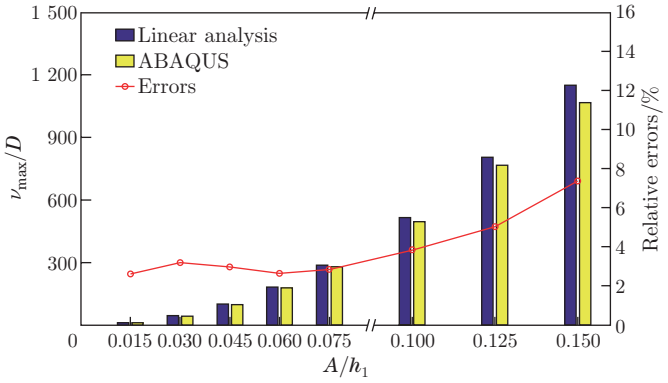

Fig. 6 Relationship between the wave amplitudes and the maximum deflection when $h_1/H = 200/700$ (color online)

The proposed method is derived based on the modal superposition method. The maximum deflections corresponding to the superposition of the first i ($i = 1, 2, 3$) mode responses are given in Fig. 8 when the maximum deflection occurs for $h_1 = 250\,\mathrm{m}$, $H = 700\,\mathrm{m}$, and $A = -15\,\mathrm{m}$. The case converges through the first three modes (generally takes the first three or four modes for a specific case).

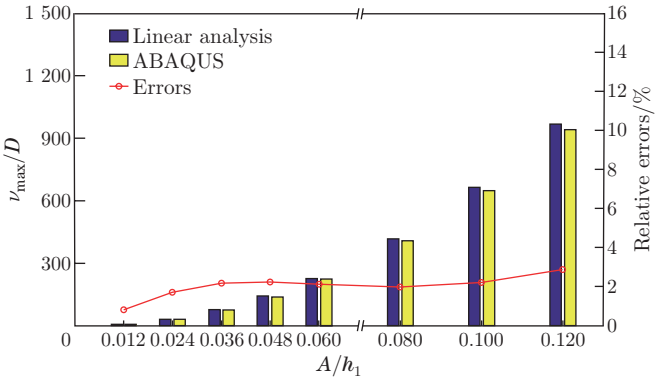

Fig. 7 Relationship between the wave amplitudes and the maximum deflection when $h_1/H = 250/700$ (color online)

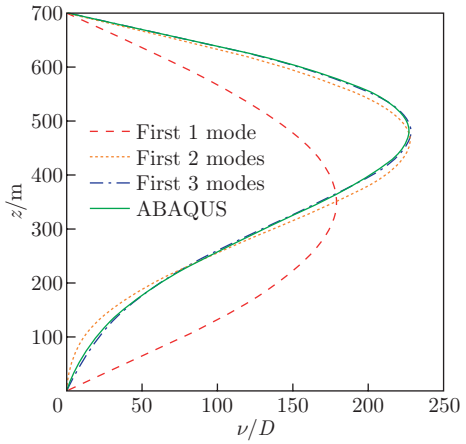

Fig. 8 Deflections corresponding to the superposition of the first i ($i = 1, 2, 3$) mode responses when the maximum deflection occurs for $h_1 = 250\,\text{m}$, $H = 700\,\text{m}$, and $A = -15\,\text{m}$ (color online)

5 Conclusions

ISWs can be a great potential threat to marine risers, because they can produce currents with a large velocity, wherein the flow directions are opposite near the pycnocline. The deflection of the marine risers arising from the ISWs is of great significance for engineering design. Fortunately, for a riser that is simply supported at its two ends, the deflection can be predicted via a linear analysis if the flow velocity induced by the ISW is obtained by means of the KdV equation for a two-layer fluid system.

For an ISW of small amplitudes, the explicit analytical expressions of the deflection and the moment of the simply supported riser are derived by means of the modal superposition method. It is found that the accuracy of the analytical expressions depends on the amplitude of the ISW. Moreover, the relative error of the maximum riser deflection obtained by the linear analysis method and the nonlinear numerical simulation is less than 6% if $A/h_1 < 0.1$, and the analytical expressions can be used for A/h_1 up to 0.2 with the tolerance of relative error 15%. Therefore, it can be concluded that the linear analysis can provide a feasible way to roughly predict the nonlinear dynamic response of a simply supported riser under an ISW with rather small amplitudes.

Conflict of interest The authors declare no conflict of interest.

References

[1] APEL, J. R., HOLBROOK, J. R., LIU, A. K., and TSAI, J. J. The Sulu Sea internal soliton experiment. *Journal of Physical Oceanography*, **15**(12), 1625–1651 (1985)

[2] OSBORNE, A. R. and BURCH, T. L. Internal solitons in the Andaman Sea. *Science*, **208**(4443), 451–460 (1980)

[3] BOLE, J. B., EBBESMEYER, C. C., and ROMEA, R. D. Soliton currents in the South China Sea: measurements and theoretical modeling. *Offshore Technology Conference*, OnePetro, Houston, USA, 2–5 (1994)

[4] CAI, S. Q., LONG, X. M., and GAN, Z. J. A method to estimate the forces exerted by internal solitons on cylindrical piles. *Ocean Engineering*, **30**(5), 673–689 (2003)

[5] CAI, S. Q., WANG, S. G., and LONG, X. M. A simple estimation of the force exerted by internal solitons on cylindrical piles. *Ocean Engineering*, **33**(7), 974–980 (2006)

[6] XIE, J. S., XU, J. X., and CAI, S. Q. A numerical study of the load on cylindrical piles exerted by internal solitary waves. *Journal of Fluids & Structures*, **27**(8), 1252–1261 (2011)

[7] LÜ, H. B., XIE, J., XU, J., CHEN, Z., LIU, T., and CAI, S. Force and torque exerted by internal solitary waves in background parabolic current on cylindrical tendon leg by numerical simulation. *Ocean Engineering*, **114**, 250–258 (2016)

[8] SONG, Z. J., TENG, B., GOU, Y., LU, L., SHI, Z. M., XIAO, Y., and QU, Y. Comparisons of internal solitary wave and surface wave actions on marine structures and their responses. *Applied Ocean Research*, **33**(2), 120–129 (2011)

[9] GUO, H., ZHANG, L., LI, X., and LOU, M. Dynamic responses of top tensioned riser under combined excitation of internal solitary wave, surface wave and vessel motion. *Journal of Ocean University of China*, **12**(1), 6–12 (2013)

[10] FAN, H., LI, C., WANG, Z., XU, L., WANG, Y., and FENG, X. Dynamic analysis of a hang-off drilling riser considering internal solitary wave and vessel motion. *Journal of Natural Gas Science and Engineering*, **37**, 512–522 (2017)

[11] LOU, M., TONG, B., and WANG, Y. Dynamic response of steel catenary riser in an internal wave field. *Journal of Offshore Mechanics & Arctic Engineering*, **140**(5), 051705 (2018)

[12] HELFRICH, K. R. and MELVILLE, W. K. Long nonlinear internal waves. *Annual Review of Fluid Mechanics*, **38**(1), 395–425 (2006)

[13] MILES, J. W. On internal solitary waves. *Tellus*, **31**(5), 456–462 (1979)

[14] CHOI, W. and CAMASSA, R. Fully nonlinear internal waves in a two-fluid system. *Journal of Fluid Mechanics*, **396**, 1–36 (1999)

[15] MORISON, J. R., JOHNSON, J. W., and SCHAAF, S. A. The force exerted by surface waves on piles. *Journal of Petroleum Technology*, **2**(5), 149–154 (1950)

[16] ZHAO, W., HUANG, X., and TIAN, J. A new method to estimate phase speed and vertical velocity of internal solitary waves in the South China Sea. *Journal of Oceanography*, **68**(5), 761–769 (2012)